

## Two Polymorphs of (Anilinium)(18-Crown-6)[Ni(dmit)<sub>2</sub>]: Structure and Magnetic Properties

Sadafumi Nishihara,<sup>\*</sup> Tomoyuki Akutagawa,<sup>\*,†</sup> Tatsuo Hasegawa,<sup>\*,†</sup> Shigeki Fujiyama,<sup>‡</sup>  
Toshikazu Nakamura,<sup>‡</sup> and Takayoshi Nakamura<sup>\*,†,1</sup>

<sup>\*</sup>Graduate School of Environmental Earth Science, Hokkaido University, Sapporo 060-0810, Japan; <sup>†</sup>Research Institute for Electronic Science, Hokkaido University, Sapporo 060-0812, Japan; and <sup>‡</sup>Institute for Molecular Science, Okazaki 444-8585, Japan

Received February 6, 2002; in revised form April 10, 2002; accepted April 12, 2002

Two polymorphs of monovalent [Ni(dmit)<sub>2</sub>]<sup>−</sup> (dmit<sup>2−</sup> = 2-thioxo-1,3-dithiole-4,5-dithiolate) crystals A and B, (anilinium)(18-crown-6)[Ni(dmit)<sub>2</sub>], were prepared, and the structure and magnetic properties were investigated. In these crystals, the [Ni(dmit)<sub>2</sub>]<sup>−</sup> molecules form dimers, which arranged into chains between the supramolecular cation structure (anilinium)(18-crown-6). In crystal A, supramolecular cation formed a regular stack, inducing ladder structure of [Ni(dmit)<sub>2</sub>], whose magnetism had been well fitted by spin ladder equation with the spin gap of  $\Delta = 190$  K. Crystal B is ca. 3% more densely packed compared to crystal A. Due to the dense packing, supramolecular cation stack is distorted, which prevented the intermolecular interaction between [Ni(dmit)<sub>2</sub>]<sup>−</sup> dimers in direction corresponds to the ladder-leg direction in crystal A. Reflecting the [Ni(dmit)<sub>2</sub>]<sup>−</sup> arrangement, crystal B showed a temperature dependence of magnetic susceptibility well reproduced by the singlet–triplet thermal activation model, whose antiferromagnetic exchange interaction ( $2J$ ) was 140 K. © 2002 Elsevier Science (USA)

**Key Words:** [Ni(dmit)<sub>2</sub>]; polymorph; spin ladder; magnetic properties; crystal structure; supramolecular cation; 18-crown-6.

### INTRODUCTION

Partially charged [Ni(dmit)<sub>2</sub>]<sup>− $\delta$</sup>  ( $\delta < 1$ , dmit<sup>2−</sup> = 2thioxo-1,3-dithiole-4,5-dithiolate) complexes provide high electrical conductivity in the molecular solids through forming one-dimensional columnar structure (1–3). While, monovalent crystals of [Ni(dmit)<sub>2</sub>]<sup>−</sup> sometimes exhibit peculiar magnetic properties, because each [Ni(dmit)<sub>2</sub>]<sup>−</sup> bears spin  $S = \frac{1}{2}$ . For example, [(CH<sub>3</sub>)<sub>4</sub>N][Ni(dmit)<sub>2</sub>]<sub>2</sub> shows the superconducting transition at 3.0 K and 3.2 kbar (4) and the ferromagnetic interaction is observed in the crystal of

[Fe(C<sub>5</sub>Me<sub>5</sub>)<sub>2</sub>][Ni(dmit)<sub>2</sub>] (5). In both cases, the regulation of intermolecular interaction between [Ni(dmit)<sub>2</sub>]<sup>−</sup> in the crystal is essential for obtaining desirable band structure and magnetic exchange interaction.

Recently, spin ladders, especially even-leg spin ladders, are attracting much attention. Even-leg ladders of  $S = \frac{1}{2}$  Heisenberg antiferromagnetic spins are in resonating valence bond state at low temperature and have a finite spin gap (6–10). It is expected that hole doping to two-leg spin ladders will lead to the superconductivity due to that effective attraction between extra holes may arise from the magnetic interactions (11). In fact, hole-doped spin ladders of copper-oxide-based materials have been reported, which exhibited superconducting transitions by chemical doping and under high pressure (12–14), or in the field-effect-transistor configuration (15).

The attempts for constructing spin ladder systems by utilizing organic radical species have been also reported by several groups (16–20). In the crystals, appropriate molecular arrangements are necessary to realize the spin ladder structure. The guiding principles for the regulation of molecular arrangements are, however, rarely known at present. We have been studying on the control of molecular assembly of [Ni(dmit)<sub>2</sub>]<sup>−</sup> in the crystals by introducing supramolecular cations composed of metal ions and crown ethers as a counter-cation of anionic [Ni(dmit)<sub>2</sub>]<sup>−</sup> species (21–23). The [Ni(dmit)<sub>2</sub>]<sup>−</sup> can interact with adjacent molecules not only through  $\pi$ – $\pi$  interaction in face-to-face manner but also through S–S atomic contacts in side-by-side direction (24–25). Therefore, [Ni(dmit)<sub>2</sub>]<sup>−</sup> is one of the best building blocks for constructing three-dimensional spin array.

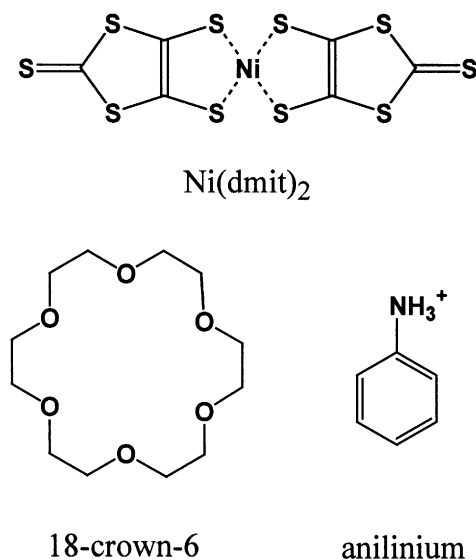
In the previous study, we succeeded in inducing [Ni(dmit)<sub>2</sub>]<sup>−</sup> ladder structure by using newly designed supramolecular cation structure (anilinium)(18-crown-6) (26). The [Ni(dmit)<sub>2</sub>]<sup>−</sup> species tend to form face-to-face

<sup>1</sup>To whom correspondence should be addressed. Research Institute for Electronic Science, Hokkaido University, Sapporo 060-0812, Japan. Fax: +81-11-706-4972. E-mail: tnaka@imd.es.hokudai.ac.jp.



dimer structure due to the energy gain of antiferromagnetic spin–spin interaction. In the crystal of (anilinium)(18-crown-6)[Ni(dmit)<sub>2</sub>] (**A**), the dimers are arranged in one dimension to form dimer chain structure by the aid of the supramolecular cation. The dimer chain exhibited a magnetic property of spin ladder because of relatively strong interdimer magnetic exchange interaction in the ladder-leg direction.

In the present paper, we will describe newly obtained polymorph, the crystal **B**. In this crystal, the arrangement of supramolecular cation is slightly changed with respect to crystal **A**, which largely affect the [Ni(dmit)<sub>2</sub>]<sup>−</sup> arrangement and the magnetic properties. (Scheme 1).



SCHEME 1.

## EXPERIMENTAL

### Preparation of Crystals

Crystals **A** and **B** were prepared by slow diffusion between (anilinium)(BF<sub>4</sub>)/18-crown-6 and (tetrabutylammonium)[Ni(dmit)<sub>2</sub>] in acetonitrile solution. Black blocks up to 2 mm<sup>3</sup> were obtained. Both the crystals were grown in the same batch and we distinguished these crystals by X-ray crystal analysis.

### X-Ray Crystal Analysis

An automated Rigaku RAXIS-RAPID diffractometer with graphite-monochromated MoK $\alpha$  radiation ( $\lambda = 0.71069 \text{ \AA}$ ) was used for data collection at 296 K. The data were corrected for Lorentz and polarization

effects, and an absorption correction was applied. The data-correct conditions and crystal data are summarized in Table 1. The crystal structures were solved by a direct method (SIR 92<sup>27</sup>), and the positions of all the hydrogen atoms were placed at the calculated ideal positions. A full-matrix least-squares technique (teXsan<sup>28</sup>) with anisotropic thermal parameters for non-hydrogen atoms and isotropic ones for hydrogen atoms was employed for a structure refinement.

### Magnetic Measurements

Static magnetic susceptibilities were measured in a field of 1 T on a Quantum Design MPMS-XL SQUID susceptometer. The temperature dependence of the magnetic susceptibility was measured in the range of 5–350 K. The magnetic susceptibilities ( $\chi$ ) of crystals **A** and **B** were deduced from impurity Curie component, which were estimated to be  $C = 0.0060$  and  $0.0011 \text{ emu K mol}^{-1}$  for crystals **A** and **B**, respectively.

## RESULTS

### Crystal Structure

Figure 1 shows the crystal structure of crystal **A**. The supramolecular cations stack regularly along the *c*-axis forming a channel-like structure. In the supramolecular

**TABLE 1**  
Data Collection and Refinement Parameters  
for Crystals **A** and **B**

	Crystal <b>A</b> <sup>a</sup>	Crystal <b>B</b> <sup>b</sup>
Crystal formula	NiS <sub>10</sub> C <sub>24</sub> NH <sub>32</sub> O <sub>6</sub>	NiS <sub>10</sub> C <sub>24</sub> NH <sub>32</sub> O <sub>6</sub>
<i>F</i> <sub>w</sub> (g)	809.82	809.82
Space group	<i>P</i> $\bar{1}$ (no. 2)	<i>P</i> $\bar{1}$ (no. 2)
Unit-cell parameters, $\text{\AA}$ and deg	<i>a</i> = 14.217(1)	<i>a</i> = 13.579(2)
	<i>b</i> = 16.666(2)	<i>b</i> = 12.605(2)
	<i>c</i> = 8.1271(6)	<i>c</i> = 10.660(2)
	$\alpha$ = 97.120(2)	$\alpha$ = 77.061(4)
	$\beta$ = 92.599(3)	$\beta$ = 74.670(8)
	$\gamma$ = 112.846(2)	$\gamma$ = 79.106(10)
<i>V</i> ( $\text{\AA}^3$ )	1751.6(3)	1698.5(5)
<i>Z</i>	2	2
$\rho$ (calc.) (g cm <sup>−3</sup> )	1.535	1.583
$\mu$ (MoK $\alpha$ ) (cm <sup>−1</sup> )	11.87	12.24
Reflection collected	14477	9142
Independent reflection	7594 [ <i>R</i> <sub>(int)</sub> = 0.041]	6052 [ <i>R</i> <sub>(int)</sub> = 0.056]
Data/parameters	5677/379	3907/379
<i>R</i> [ <i>I</i> > 3 $\sigma$ ( <i>I</i> )]	<i>R</i> <sub>1</sub> = 0.051	<i>R</i> <sub>1</sub> = 0.050
	<i>R</i> <sub>w</sub> = 0.167	<i>R</i> <sub>w</sub> = 0.127
Largest diff. peak and hole (e $\text{\AA}^{-3}$ )	0.37 and −0.42	0.35 and −0.51

<sup>a</sup>Ref. (26).

<sup>b</sup>CCDC #184318.

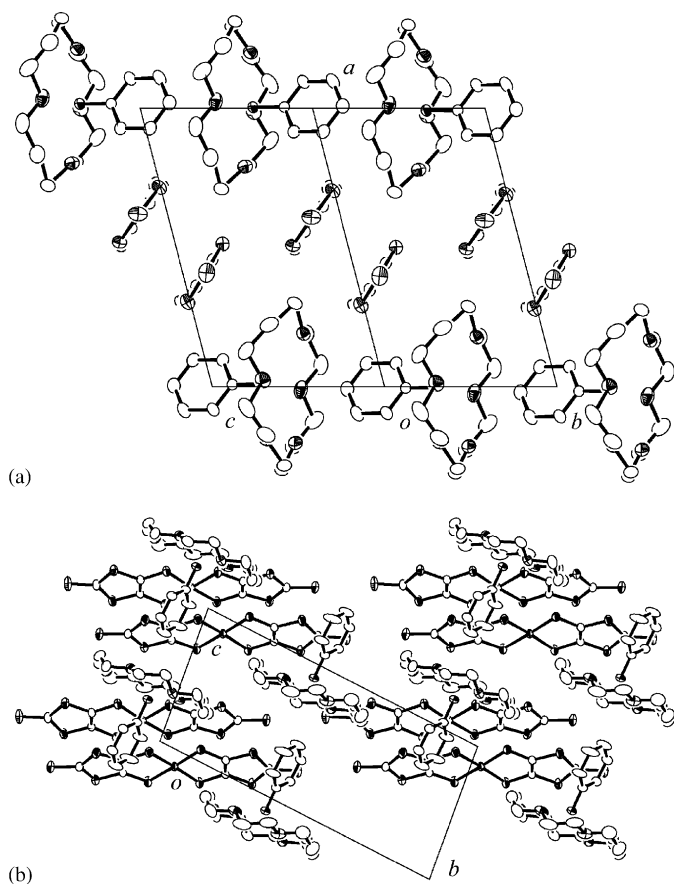


FIG. 1. Structure of crystal **A** viewed along the  $b+c$ -axis (a) and the  $a$ -axis (b).

cation structure,  $-\text{NH}_3^+$  group located at the center of 18-crown-6 cavity  $0.914(3)$  Å above the 18-crown-6 molecular plane, forming  $\text{NH}^+-\text{O}$  hydrogen bonds with oxygen atoms. The average hydrogen-bond length was  $2.92$  Å, which is slightly longer than the standard  $\text{NH}^+-\text{O}$  distance ( $2.87$  Å) (29). The  $[\text{Ni}(\text{dmit})_2]^-$  forms dimer, which are arranged into one-dimensional array guided by the ditch formed by side-by-side supramolecular cation stack in the (011) direction.

Figure 2 shows the crystal structure of crystal **B**. The individual supramolecular cation structure of (anilinium)(18-crown-6) is almost the same as that in the case of crystal **A**, with  $-\text{NH}_3^+$  group locating  $0.928(5)$  Å above the 18-crown-6 molecular plane, and with the average hydrogen-bond length of  $2.91$  Å. The significant difference in supramolecular arrangements between crystals **A** and **B** is that the molecular long axis of anilinium moiety is not parallel to the stacking axis of supramolecular cation in the latter case. Therefore, the channel-like structure of 18-crown-6 was not observed in crystal **B**. The  $[\text{Ni}(\text{dmit})_2]^-$  forms dimer and stacks along the  $b$ -axis filling the space between cationic columns.

We examined the details of supramolecular cation and  $[\text{Ni}(\text{dmit})_2]^-$  arrangements to evaluate the structural difference between crystals **A** and **B** quantitatively. Fig. 3 shows the molecular arrangements of supramolecular cations and  $[\text{Ni}(\text{dmit})_2]^-$  array in crystal **A**. The supramolecular cation stacks regularly in a head-to-tail manner with the repeating distance  $d_{A1}$  of  $8.1271(6)$  Å and the molecular axis of anilinium is almost parallel to the stacking axis. The angle  $\theta_{A1}$ , which is defined as an angle between C–N bond direction of anilinium and stacking axis (N(554)–N(555)–C(555)), is  $5.22^\circ$ . The distance between average plane of  $[\text{Ni}(\text{dmit})_2]^-$  in a dimer is  $3.65$  Å and the dimer stacked in head-to-tail manner with the repeating distance  $d_{A2} = 17.613(1)$  Å. The long axis of  $[\text{Ni}(\text{dmit})_2]^-$  makes an angle of  $1.28^\circ$  with the dimer stacking direction ( $\text{S3}(555)\text{--}\text{S3}(566)\text{--}\text{S8}(566) = 1.28^\circ$ ).

We calculated the transfer integrals to estimate the intermolecular interaction between  $[\text{Ni}(\text{dmit})_2]^-$  by the extended Hückel molecular orbital calculation (30). The strongest interaction  $t_{A1} = 45.3$  meV was observed within the dimer, which corresponds to the ladder-rung direction. The second strongest is that in ladder-leg direction,

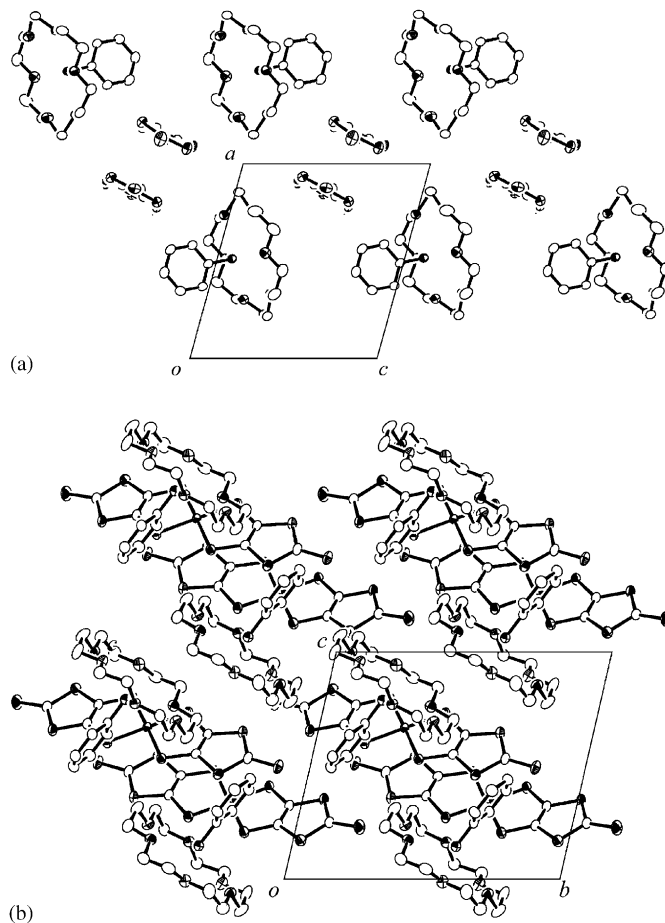


FIG. 2. Structure of crystal **B** viewed along the  $b$ -axis (a) and  $a$ -axis (b).

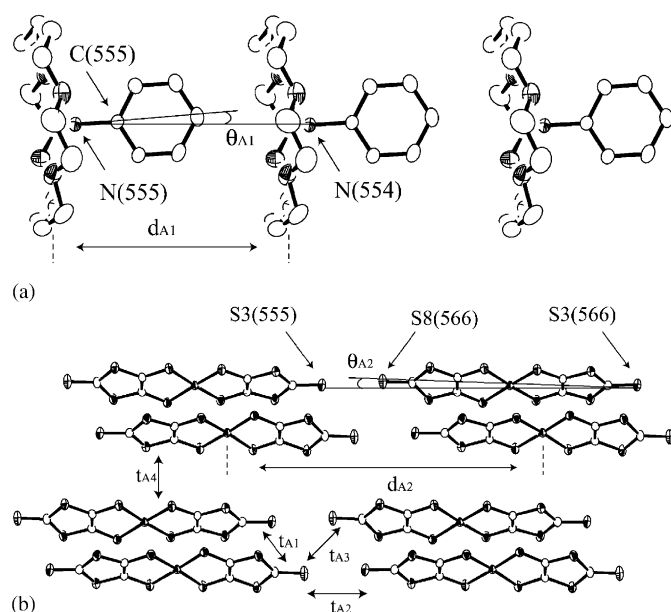


FIG. 3. Structure of supramolecular array (a) and  $[\text{Ni}(\text{dmit})_2]^-$  arrangement (b) in the crystal A.

$t_{A2} = 15.9$  meV, and  $t_{A3} = 11.3$  meV in the diagonal direction is also observed. Relatively large interaction  $t_{A4} = 10.6$  meV exists between ladders.

Figure 4 depicted the molecular arrangements in crystal B. Although the supramolecular cation part stacks

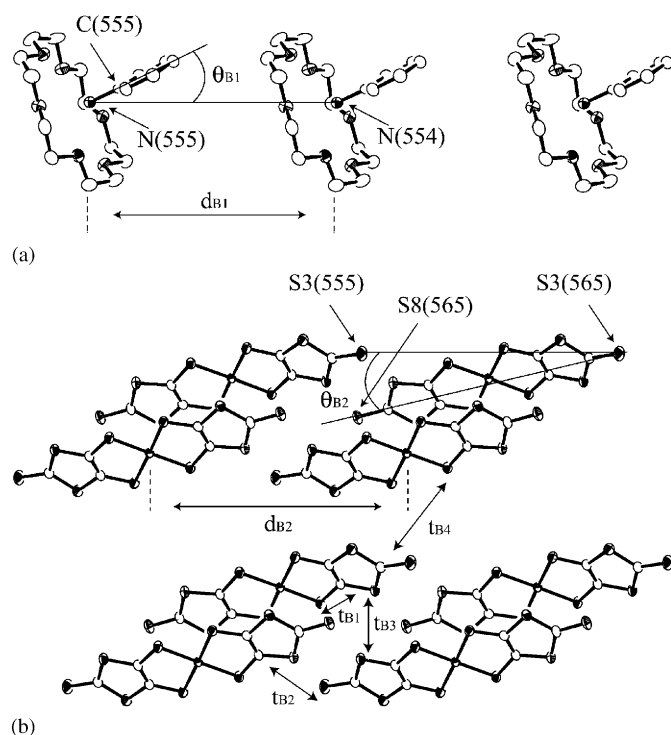


FIG. 4. Structure of supramolecular array (a) and  $[\text{Ni}(\text{dmit})_2]^-$  arrangement (b) in the crystal B.

regularly along the  $c$ -axis with the repeating distance of  $d_{B1} = 10.660(2)$  Å, the molecular long axis of anilinum does not parallel to the stacking direction as seen in Fig. 4a. The angle  $\theta_{B1}$  (N(554)–N(555)–C(555)) is  $31.39^\circ$ , which is quite large compared to that of crystal A. The long axis of  $[\text{Ni}(\text{dmit})_2]^-$  also forms an angle  $\theta_{B2} = 24.61^\circ$  (S3(555)–S3(565)–S8(565)) with  $[\text{Ni}(\text{dmit})_2]^-$  dimer stacking direction. Accordingly, the repeating distance of the  $[\text{Ni}(\text{dmit})_2]^-$  dimer along the stacking axis,  $d_{B2} = 12.605(2)$  Å is much shorter than that of crystal A.

The distance between average plane of  $[\text{Ni}(\text{dmit})_2]^-$  within a dimer is  $3.33$  Å, quite shorter than that seen in crystal A. However, the intermolecular interaction estimated from transfer integral is comparable ( $t_{B1} = 48.0$  meV). On the other hand, the interaction between the dimer within a chain is negligible, showing a keen difference with the ladder structure in crystal A. The interaction in the diagonal direction and between chains are  $t_{B3} = 18.5$  meV and  $t_{B4} = 6.7$  meV, respectively. The transfer integrals together with the typical intermolecular distances and angles are summarized in Table 2.

### Magnetic Properties

Figure 5 shows the temperature dependence of the magnetic susceptibility of crystal B. The results of crystal A is also indicated for the comparison. The curves in Fig. 5 are the results of the fits. As reported previously, the magnetic behavior of crystal A is well explained by the spin ladder model (31) with the spin gap ( $\Delta$ ) of  $190$  K.

The temperature dependence of the nuclear spin-lattice relaxation rate ( $1/T_1$ ) in  $^1\text{H}$ -NMR was measured on crystal A in the range of  $1.6$ – $268$  K. The exponential decrease  $1/T_1$  below  $50$  K was observed which is consistent with the presence of the spin gap suggested from SQUID measure-

TABLE 2  
Typical Intermolecular Distances and Angles in the Crystals and Intermolecular Interaction

	Crystal A	Crystal B
Distance (Å)		
$d_1$	8.1271(6)	10.660(2)
$d_2$	17.613(1)	12.605(2)
Angle (deg)		
$\theta_1$	5.22	31.39
$\theta_2$	1.28	24.61
Transfer integral (meV)		
$t_1$	45.3	48.0
$t_2$	15.9	0
$t_3$	11.3	18.5
$t_4$	10.6	6.7

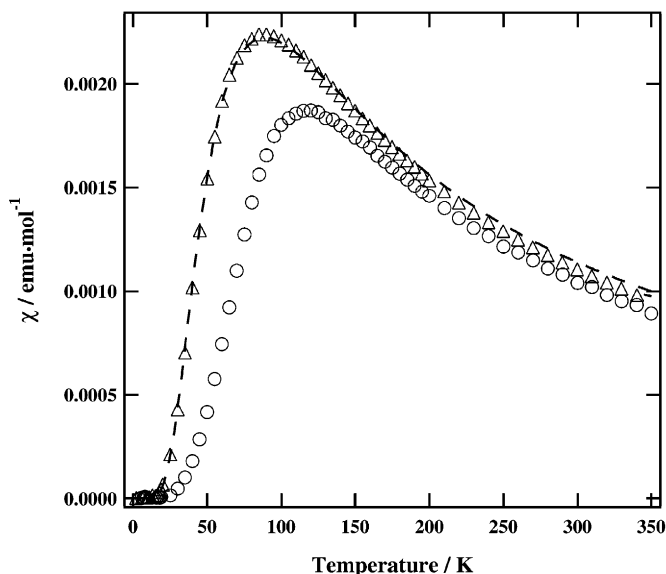


FIG. 5. Temperature dependence of the magnetic susceptibility of crystal **A** (○) and **B** (△) together with the fitting curve (see text).

ment. The details of the <sup>1</sup>H-NMR measurements will be reported separately (32).

The magnetic behavior of crystal **B** is similar to that of crystal **A**, showing maximum at 90 K and decreasing exponentially with the decrease in temperature below that temperature. The temperature dependence of the susceptibility in the whole measuring range was, however, well explained by the ordinary singlet–triplet thermal activation model,

$$\chi_{\text{singlet-triplet}} = \frac{C}{T} \frac{4\exp(-2J/T)}{1 + 3\exp(-2J/T)}, \quad [1]$$

using  $C = 0.394 \text{ emu K mol}^{-1}$ . The best fit indicated by the dashed curve in Fig. 5 obtained with the antiferromagnetic exchange interaction of  $2J = 140 \text{ K}$ . Because the transfer integral in the dimer-chain direction in crystal **B** is negligible, it is quite reasonable that we could not observe the spin ladder behavior in crystal **B**. Considering relatively large interdimer interaction ( $t_{B3} = 18.5 \text{ meV}$ ) in the diagonal direction, we also applied alternate Heisenberg model for crystal **B**. The  $\alpha$  value obtained by the fit was 0.03, showing that dimers in crystal **B** is rather isolated.

## DISCUSSION

The two polymorphs of (anilinium)(18-crown-6)[Ni(dmit)<sub>2</sub>] showed different magnetic behavior reflecting the molecular arrangements in each crystal. We discuss here how the small modification in the crystal structure leads to a large difference in magnetic properties. The unit-cell volume of crystal **B** is about 3% smaller than that of crystal

**A**. Due to the dense packing, the molecular arrangement as well as the conformation of individual molecule are somewhat distorted in crystal **B** compared with those of crystal **A**.

Figure 6 shows schematic representation of relative arrangements of supramolecular cations and [Ni(dmit)<sub>2</sub>]<sup>−</sup> in the crystals. In crystal **A**, the supramolecular cation represented by cones is stacked regularly with their apex in the stacking direction. The cone also stacks side-by-side and forms the space where [Ni(dmit)<sub>2</sub>]<sup>−</sup> dimer can develop a chain structure in the direction orthogonal to the cone-stack.

In crystal **B**, although the structure of each supramolecular cation (cone) is almost the same as in crystal **A**, the direction of the apex is not parallel to the stacking direction and, therefore, distorted supramolecular chain structure is observed. The distortion, which is probably due to the dense packing of the molecules in the crystal, induces the distortion in dimer chain structure of [Ni(dmit)<sub>2</sub>]<sup>−</sup>.

The distortion in supramolecular cation array also causes the large change within the dimer structure. As mentioned before, the intradimer distance between average plane of [Ni(dmit)<sub>2</sub>]<sup>−</sup> in crystal **B** is 3.33 Å, about 0.3 Å shorter than that in crystal **A**. Such short distance should result in very strong intermolecular interaction. However, the intradimer interaction is comparable with that in crystal **A** from transfer integral calculation and magnetic measurements. The origin of this small intradimer interaction in crystal **B** is explained as follows.

The [Ni(dmit)<sub>2</sub>]<sup>−</sup> has a distorted structure in crystal **B**. The dihedral angles between two planes formed by dmit ligands are 174.9° and 171.4°, respectively, for crystals **A** and **B**. Since the interplanar distances were defined from an average plane of [Ni(dmit)<sub>2</sub>]<sup>−</sup> molecules obtained by the least-squares method. Although the calculation gives a very accurate value when a molecule is almost planar as in the case of crystal **A**, the error is relatively large for a bent molecule in crystal **B**. Therefore, we calculated intermolecular distance by a different method for crystal **B**. As seen in Fig. 4, longer offset in longitudinal direction is observed upon forming dimer in crystal **B**, and one of the dmit ligand of each molecule is overlapping and almost parallel within the dimer. The interplanar distance between two ligands is 3.64 Å, which is comparable to interplanar distance of 3.65 Å within the dimer in crystal **A**.

In crystal **A**, the longitudinal offset is 1.8(1) Å, while that in crystal **B** is 4.2(1) Å. The larger offset generally results in a less efficient overlapping of LUMO. However, five short S...S contacts shorter than 4.00 Å were observed in crystal **B**, which results in the efficient intermolecular interaction comparable with that in crystal **A** with four short S...S contacts within a dimer.

The longer molecular offset within the dimer also causes a large change in interdimer interaction in crystal **B**. For

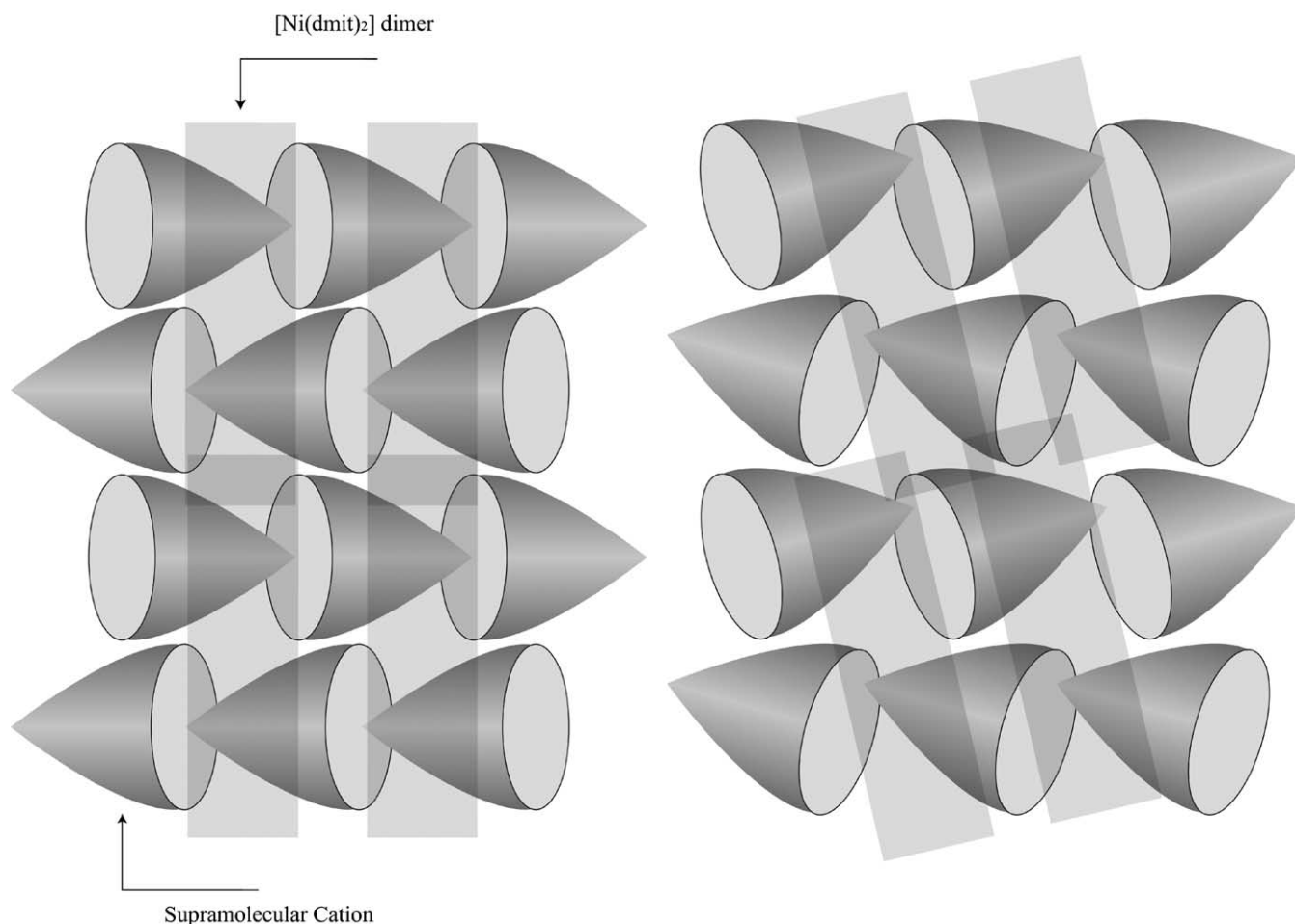


FIG. 6. Schematic representation of supramolecular cation and  $[\text{Ni}(\text{dmit})_2]^-$  arrangements in crystals **A** (a) and **B** (b).

example, the interaction in the diagonal direction ( $t_{B3}$ ) is twice as large as that of crystal **A** ( $t_{A3}$ ). In crystal **B**, each  $[\text{Ni}(\text{dmit})_2]^-$  has a large portion at the molecular end through which stronger interaction in diagonal direction is possible between the dimers. The largest change in intermolecular interaction from crystals **A** to **B** is, however, observed in  $t_2$ , which is responsible for asserting spin ladder magnetism. As is seen in Fig. 6b, each  $[\text{Ni}(\text{dmit})_2]^-$  dimer forms a large angle with respect to the chain direction due to the dense packing of supramolecular cation in crystal **B**. As a result, ladder-type interdimer interaction is impossible in the crystal.

### CONCLUSION

In this study, we described two polymorphs of (anilinium)(18-crown-6) $[\text{Ni}(\text{dmit})_2]$  crystals **A** and **B**. The small change in supramolecular array induced the large change in  $[\text{Ni}(\text{dmit})_2]^-$  dimer stack structure and magnetism. The regular dimer chain structure in crystal **A** gave a spin

ladder, whereas the magnetic properties of distorted dimer chain in crystal **B** was well explained by the ordinary singlet–triplet thermal excitation model. These magnetisms were discussed in terms of intermolecular interactions between  $[\text{Ni}(\text{dmit})_2]^-$ . These results indicate a large effect on  $[\text{Ni}(\text{dmit})_2]^-$  assembly structure from supramolecular cation. The results also strongly suggest that through appropriate design of supramolecular cation, it is possible to regulate  $[\text{Ni}(\text{dmit})_2]^-$  assembly and, therefore, the magnetism arising from the assembly. The formation of ideal spin ladder structure and investigation of novel magnetic properties from these approaches are now underway.

Another interesting point associated with the spin ladder structure is the carrier doping, through which superconducting transition at relatively high temperature is expected. One possible way is to replace a portion of anilinium to aniline in the crystal, which will be carried out without large distortion in  $[\text{Ni}(\text{dmit})_2]^-$  array within the crystal.

## ACKNOWLEDGMENTS

The authors thank Dr. K. Ichimura and Prof. K. Nomura for the use of the SQUID magnetometer. This work was partly supported by a Grant-in-Aid for Science Research from the Ministry of Education, Culture, Sports, Science and Technology of Japan and by the Proposal-Based New Industry Creative Type Technology R&D Promotion Program from the New Energy and Industrial Technology Development Organization (NEDO) in Japan.

## REFERENCES

1. L. Alcácer and H. Novais, "Extended Linear Chain Compounds" in (J. S. Miller, Ed.), Vol. 3, p. 319. Plenum Press, New York, 1983.
2. P. Cassoux, L. Valade, H. Kobayashi, A. Kobayashi, R. A. Clark, and A. E. Underhill, *Coord. Chem. Rev.* **110**, 115 (1991).
3. "Handbook of Organic Conductive Molecules and Polymers," (H. S. Nalwa, Ed.) Vol. 1. John Wiley & Sons, Chichester, UK, 1997.
4. H. Kim, A. Kobayashi, Y. Sasaki, R. Kato, and H. Kobayashi, *Chem. Lett.* 1799 (1987)
5. W. E. Broderich, J. A. Thompson, M. R. Godfrey, M. Sabat, and B. M. Hoffman, *J. Am. Chem. Soc.* **111**, 7656 (1989).
6. P. W. Anderson, *Science* **235**, 1196 (1987).
7. E. Dagotto and T. M. Rice, *Science* **271**, 618 (1996).
8. D. C. Johnston, J. W. Johnson, D. P. Goshorn, and A. J. Jacobson, *Phys. Rev. B* **35**, 219 (1987).
9. T. M. Rice, S. Gopalan, and M. Sigrist, *Europhys. Lett.* **23**, 445 (1993).
10. D. J. Scalapino, *Nature* **377**, 12 (1995).
11. J. C. Bonner and M. E. Fisher, *Phys. Rev. B* **14**, 3036 (1976).
12. M. Maekawa, *Science* **273**, 1515 (1996).
13. Z. Hiroi and M. Takano, *Nature* **377**, 41 (1995).
14. M. Uehara, T. Nagata, J. Akimitsu, H. Takahashi, N. Mori, and K. Kinoshita, *J. Phys. Soc. Jpn.* **65**, 2764 (1996).
15. J. H. Schön, M. Dorget, F. C. Beuran, X. Z. Xu, E. Arushanov, M. Lagues, and C. Deville Cavellin, *Science* **293**, 2430 (2001).
16. C. Rovira, *Chem. Eur. J* **6**, 1723 (2000).
17. C. Rovira, J. Veciana, E. Ribera, J. Tarrés, E. Candell, R. Rousseau, M. Mas, E. Molins, M. Almeida, R. T. Henriques, J. Morgado, J. P. Schoeffel, and J. P. Pouget, *Angew. Chem.* **109**, 2418 (1997).
18. H. Imai, T. Inabe, T. Otsuka, T. Okuno, and K. Awaga, *Phys. Rev. B* **54**, R6338 (1996).
19. T. Komatsu, N. Kojima, and G. Saito, *Solid State Commun.* **103**, 519 (1997).
20. M. Fourmigué, B. Domerq, I. V. Jourdain, P. Molinié, F. Guyon, and J. Amaudrut, *Chem. Eur. J* **4**, 1714 (1988).
21. N. Takamatsu, T. Akutagawa, T. Hasegawa, T. Nakamura, T. Inabe, W. Fujita, and K. Awaga, *Inorg. Chem.* **39**, 870 (2000).
22. T. Akutagawa, S. Nishihara, N. Takamatsu, T. Hasegawa, T. Nakamura, and T. Inabe, *J. Phys. Chem. B* **104**, 5871 (2000).
23. S. Nishihara, N. Takamatsu, T. Akutagawa, T. Hasegawa, and T. Nakamura, *Synth. Met.* **121**, 1806 (2001).
24. W. B. Heuer, A. E. True, P. N. Swepston, and B. M. Hoffman, *Inorg. Chem.* **27**, 1474 (1988).
25. W. B. Heuer, P. J. Squattrito, B. M. Hoffman, and J. A. Ibers, *J. Am. Chem. Soc.* **110**, 792 (1988).
26. S. Nishihara, T. Akutagawa, T. Hasegawa, and T. Nakamura, *Chem. Commun.* 408 (2002).
27. A. Altomare, M. C. Burla, M. Camalli, M. Cascarano, C. Giacovazzo, A. Guagliardi, and G. Polidori, *J. Appl. Crystallogr.* **27**, 435 (1994).
28. "teXsan: Crystal Structure Analysis Package." Molecular Structure Corporation, 1985 and 1992.
29. G. C. Pimentel and A. L. McClellan, "The Hydrogen Bond." Freeman, San Francisco, CA, 1960.
30. T. Mori, A. Kobayashi, Y. Sasaki, H. Kobayashi, G. Saito, and H. Inokuchi, *Bull. Chem. Soc. Jpn.* **57**, 627 (1984).
31. M. Troyer, H. Tsunetsugu, and D. Würtz, *Phys. Rev. B* **50**, 13,515 (1994).
32. S. Nishihara, T. Akutagawa, T. Hasegawa, T. Nakamura, S. Fujiyama, and T. Nakamura, *Synth. Met.*, submitted.